6-DoFs MEMS-based precision manipulator

Combining Design Principles, a mature design philosophy for creating precision machines, and MEMS fabrication, a technology for miniaturization, could lead to micro systems with deterministic behavior and accurate positioning capability. However, in MEMS design trade-offs need to be made between fabrication complexity and design principle requirements. Here a micro-mechatronic design of a Stewart Platform, a six Degrees-of-Freedom MEMS-based Precision Manipulator, is presented.

• *Dannis Brouwer and Herman Soemers* •

In the future, the precision manipulation of small objects will become more and more important for appliances such as (probe-based) data storage, micro assembly, sample manipulation in microscopes, cell manipulation, nano indenting, manipulation of optical beam paths by micro mirrors and manipulation of E-beam paths by phase plates. At the same time, there is a drive towards miniaturized systems. An example can be found in the manipulation of samples in a transmission electron microscope (TEM). The relatively large dimensions of ‘conventional’ TEM sample manipulators result in typical drawbacks such as thermal drift and compromised dynamics. Especially the requested stability of 0.1 nm/min requires a new manipulator concept.

Miniaturization creates the opportunity to fix the manipulator directly to the column which guides the electron beam, isolating external thermal and vibration noise. Secondly miniaturizing the manipulator generally results in enhanced stability because of increased natural frequencies, decreased thermal drift and in small thermal time constants of the manipulator. Potential solutions for miniaturizing can be found in Micro Electro Mechanical Systems (MEMS). MEMS devices comprise micro sensors, actuators, mechanisms, optics and fluidic systems. They have the ability to integrate several functions in a small package. Precision manipulation in MEMS seems sparse however. E. Sarajlic has fabricated a 2-DoFs MEMS-based manipulator for data storage purposes for example, as shown in Figure 1.

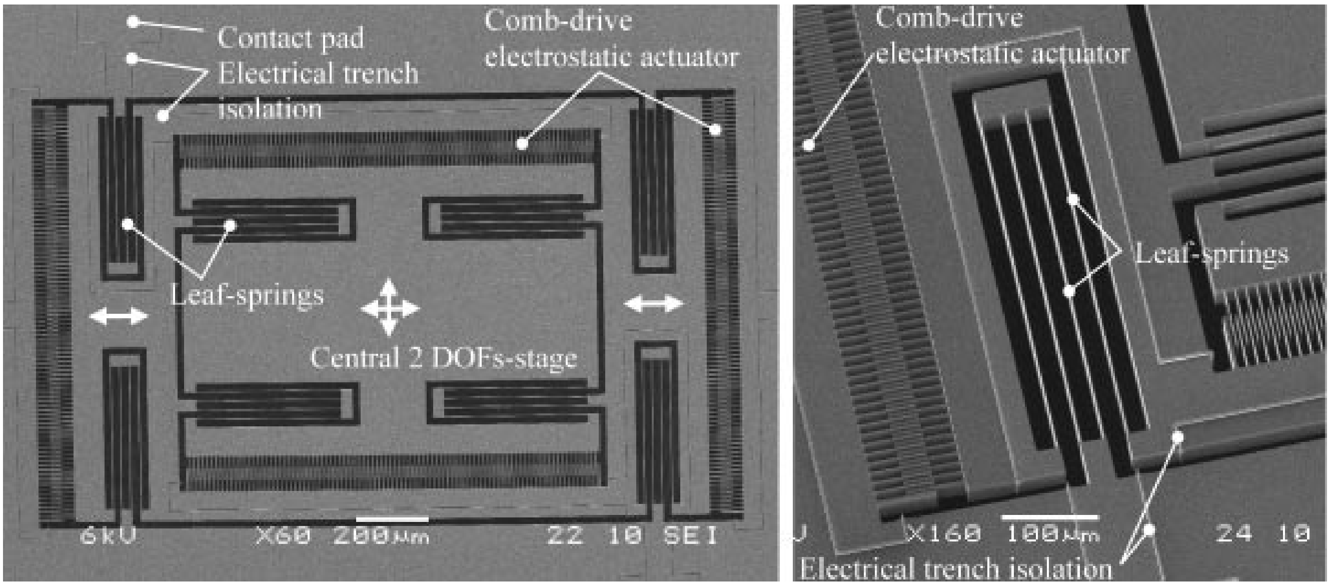

a

b

Figure 1. SEM pictures of MEMS devices (both fabricated by E. Sarajlic).
(a) 2-DoFs stacked MEMS-based manipulator (material is grey).
(b) Detail of the comb-drive electrostatic actuator and the leaf-spring suspension (often called folded flexure).

Specifications

The specifications of the manipulator are based on a next generation TEM sample manipulator. First, the manipulator has to operate in an ultra high vacuum (10^{-8} - 10^{-9} Torr) and should not interfere with the E-beam. The maximum displacement should be enough to examine a sample. A semiconductor sample is typically 20 x 10 x 0.2 μm^3. Therefore, the *x*- and *y*-strokes of the manipulator should be about 20 µm. For the focusing of the electron beam, the *z*-stroke should be about 20 µm also. Once an area of interest is found on the sample, the TEM sample manipulator should be able to find this area again with a translational repeatability of about 10 nm. Extremely fine positioning is possible by manipulating the E-beam itself. The MEMS-based manipulator will be used for small correction angles up to several degrees only. The rotational repeatability needs to be better than 0.05°.

Some TEMs can be used in a scanning TEM (STEM) mode, where the beam can be scanned across the sample to form the image. Taking a picture in the STEM mode can take up to half a minute. This fact, combined with the possible image resolution of 0.08 nm, results in an extreme stability requirement of 0.1 nm/min for the sample with respect to the E-beam. This stability should be reached within 10 s after the manipulation of the sample. Because of the high resolution capability of the TEM, sound and the vibrating surroundings cause the TEM column to vibrate, which could lead to blurred images. Therefore, the sample needs to be fixed dynamically stable to the TEM column. Therefore, a next generation manipulator requires a lowest vibration mode frequency of more than 1 kHz. A summary of the specifications is given in Table 1.

Table 1. Specifications for a next generation TEM sample manipulator.

Property	**Value**
Stroke *x*, *y*, *z*	20 µm
Repeatability *x*, *y*, *z*	10 nm
Rotational stroke (any 2 DoFs)	3°
Rotational repeatability	0.05°
Stability (within 10 s)	0.1 nm/min
First vibration mode frequency	> 1 kHz

MEMS-based Mechatronic System Design

There are some important differences between a mechatronic design in MEMS and in the macro scale world. In MEMS:

- The influence of the fabrication technology on the design is large.
- Fabrication technology is often based on planar processes.
- The influence of the actuator choice is great.
- Sensing is relatively inaccurate.
- The repeatability of compliant mechanisms in Si-based technology is extremely high.

Design Basics: Design principles and bulk micro machining fabrication technology

The design principles for precision mechanisms [1,2,3,4,5,6,7] are a design philosophy enabling or enhancing accurate maneuvering and positioning. The design principles which are especially relevant in the MEMS-based 6-DoFs manipulator design are:

- Determinism, promotes the use of compliant mechanisms (no friction, no wear, low hysteresis, no play).
- Exact kinematic constraint design.
- Symmetry.

Roughly MEMS fabrication can be subdivided into ‘bulk micro machining’ based processes [8] and ‘surface micromachining’ based processes. Surface micro machining is basically deposition and removal of relatively thin layers of material on a wafer. In bulk micro machining processes the wafer itself is etched resulting in high (out-of-wafer-plane) structures. High aspect-ratio structures, such as leaf-springs of 35-40 μm high and 2 μm thick, can be made by Deep Reactive Ion Etching (DRIE). High leaf-springs are necessary for increasing the out-of-wafer-plane stiffness of the relatively large MEMS devices. Electrical wiring in bulk micro machined devices can be done by so called trench isolation [9]. A wall of insulation material divides the silicon, resulting in isolated electrical parts. Figure 1 shows an example of trench isolation.

The derived concept is based on the design principles in combination with mainly bulk micro machining processes.

Motion in-plane and out-of-plane of the wafer

6-DoFs positioning requires both in-plane and out-of-plane motion. Basically there are two options for 6-DoFs motion generation:

- Combination of in-plane and out-of-plane actuators in one system.
- Use of a mechanism to convert in-plane to out-of-plane motion or vice versa.

Usually the technology to fabricate in-plane actuators differs from the technology to fabricate out-of-plane actuators. Therefore, a combination between the two is a rarity. Although it is easier to fabricate six actuators of the same type than three in-plane and three out-of-plane actuators, the mechanism needed to convert motion usually also requires special additional process steps. The combination of a motion converting mechanism with one type of actuator will be developed.

Actuation principle in MEMS

MEMS-based magnetic actuators have a low energy density. Piezo (PZT) actuators are difficult to integrate in MEMS technology or need assembly. Thermal actuators can have an energy density comparable to electrostatic actuators. However, to fabricate uni-morph and multi-morph actuators thin film technology is required which conflicts with integration into a bulk micro-machined system. Simple extenders have a limited stroke and require strong stroke amplification. In general, thermal actuators lack thermal stability, causing position uncertainty at nano manipulation.

Regarding the necessary stroke and force of the manipulator a lateral comb-drive electrostatic actuator, as shown in Figure 1b, would suffice. This type of actuator integrates well into bulk micro machining. Comb-drives are linear motors that utilize electrostatic forces that act between two conductor combs. In a lateral comb-drive actuator the fingers are typically arranged in such a way that they can slide past one another until each finger occupies the slot in the opposite comb. One comb is fixed and the other one is connected to a suspension with compliance in the longitudinal direction of the fingers. Applying a voltage difference between the comb structures will result in a movement by electrostatic forces in the finger direction. Six electrostatic comb-drives will be used for actuation. The problem of the interaction of the E-beam with electrostatic actuators can be overcome by either blocking the actuators with a clamp or by shielding. The typical electrostatic force per finger pair at 60 V is 0.5 µN.

In general the actuators used in MEMS exhibit low work density compared to the energy storage in elastic elements. Consequently, the actuators in MEMS are relatively large and the elastic elements are generally long and slender.

Serial versus parallel kinematic mechanism

A distinction can be made between two main basic concepts with regard to the mechanism. One type is serial, the other is parallel. In a serial mechanism, there is one kinematic chain of links and joints between the end-effector and base. A typical example of a serial manipulator is the classic assembly robot as often used in the automotive industry. In a parallel mechanism, multiple independent kinematic chains exist parallel to each other between the end-effector and the base. An example of a parallel 6-DoFs mechanism is a Stewart platform, which is often used in flight-simulators.

In MEMS a parallel mechanism can be used to convert motion from in-plane to out-of-plane. The high vibration mode frequencies in this case are convenient in the TEM application for a good coupling between the TEM column and the sample. A large advantage of a parallel set-up, especially in MEMS, is that the actuators are stationary. This makes routing of the electrical connections, generally difficult in MEMS, to the actuators (and sensors) easy.

Position control

Two specifications with respect to positioning need to be distinguished: the positional *repeatability* and the *stability*. The repeatability specified at 10 nm is the uncertainty at which the manipulator can reproduce a position each time. The stability of 0.1 nm specifies how well the position is kept constant relative to the electron beam over a certain amount of time, in this case 1 min.

Precision macro systems often rely on feedback for accurate position information. Measuring on the micro scale is less trivial. In general, measuring with an uncertainty less than 10 nm over a range of 20 µm at a sensing bandwidth of 10-100 Hz in MEMS is far from straightforward. In the TEM manipulator application there is no unknown external disturbance force loading the manipulator except for forces due to external vibrations. In addition, MEMS, especially silicon, is known for its low hysteresis, due to the monolithic and often single crystal mechanical structure. Combined with a fully compliant, no-friction mechanism the repeatability and stability of the system without feedback, only using feed-forward, can be excellent. However, because of manufacturing uncertainty the mechanism needs to be calibrated in a 6-DoFs set-up. In applications where substantial external forces exist, such as micro assembly, capacitive sensors coupled to the actuators are probably a necessity to achieve sub-micron repeatability.

Passive mechanical *stability* of the manipulator means that the manipulator depends on material properties to counteract position deterioration due to temperature fluctuations and vibrations. There are several reasons why the passive stability can be enhanced by unpowered blocking of the manipulator using a clamping mechanism once it has reached its targeted position:

- Cross-talk between the electron beam of the TEM and electric or magnetic fields from the actuators of the manipulator affects the stability of the E-beam and the manipulator. Clamping (of course without generating electric or magnetic fields) decreases this cross-talk.
- By using a clamping mechanism, the manipulator can be switched between compliant actuation modes for positioning, and high frequent vibration modes during imaging.

In the final design a mechanical clamp with a locking device is integrated.
Three different total concepts of combined fabrication and mechatronic design have been regarded. The most feasible will be explained.

The Kinematic Concept

The manipulator, which is schematically shown in Figure 2, has a flat base over which three intermediate bodies can move. Each intermediate body is actuated in two translational DoFs (*x* and *y* in Figure 2) and constrained in the other four DoFs (*z, Rx*, *Ry* and *Rz*). The ball joint connecting the intermediate body with the triangle releases three DoFs. The triangle has two actuated, three free and one constrained DoFs therefore. The hinge releases another DoF. Therefore, the platform has two actuated and four free DoFs by one leg as shown in Figure 2. Table 2 summarizes the DoFs per leg.

Table 2. The DoFs of the rigid bodies of one leg of the manipulator.

	Free	Actuated	Constrained
Intermediate body	0	2	4
Triangle	3	2	1
Platform	4	2	0

Ball joint releases three DoFs

Hinge releases one DoF

The combination of three times two DoFs actuated per leg results in the platform having six DoFs actuated. Each of the individual DoFs of the platform is shown with the corresponding intermediate body *xy*-translations in Figure 3.

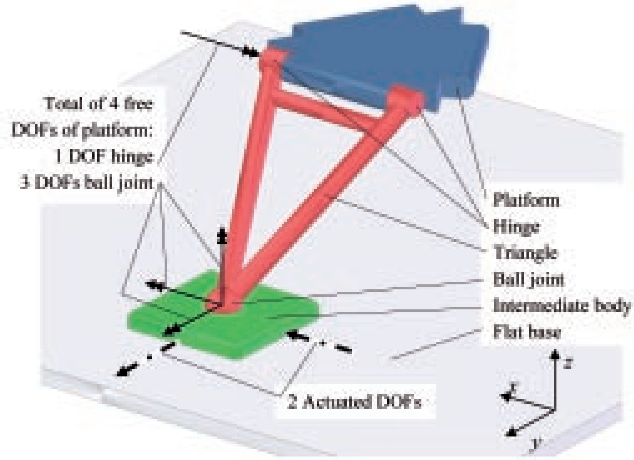

Figure 2. One of the three legs of the manipulator with the platform. The six DoFs of the platform, four free and two actuated, are indicated by the six arrows.

The kinematic concept as implemented in the MEMS-based manipulator, shown in Figure 4, is almost equivalent to the kinematic concept shown in Figure 2. Two Si-leaf-springs, which are connected at the intermediate body, leave one DoF compliant, the rotation around their intersection. The slanted leaf-spring releases three DoFs, which can be regarded as three rotational DoFs, as shown in Figure 4. The three compliant DoFs near the intermediate body can be regarded as a ball joint, equivalent to the ball joint in Figure 2. Although these three rotational compliant DoFs are not orthogonal, they do act as an elastic ball joint, because they do not coincide, are not parallel and intersect close to each other. The compliant DoF near the platform can be regarded as the hinge equivalent of Figure 2. The combination of three times two DoFs actuated per leg results in the platform having six DoFs actuated (Figure 5). To give an impression of the dimensions: the overall size is 4.9 x 5.2 mm^2. The platform is elevated 460 μm above the comb-drives, folded flexures and Si-leaf-springs. Because of anisotropic etching along crystal planes of the silicon, which is used for obtaining the slanted leaf-springs, a 90° angle between the slanted leaf-springs results.

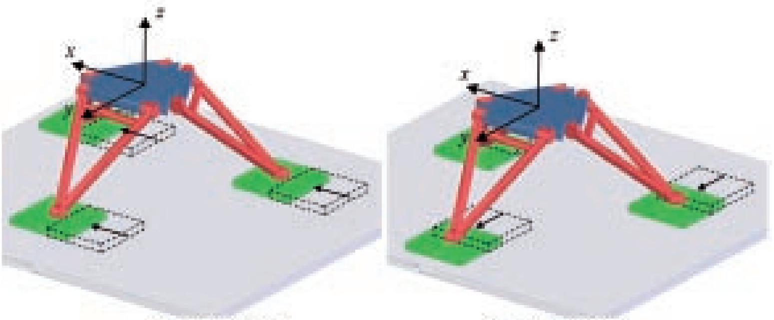

(a) x-translation (b) y-translation

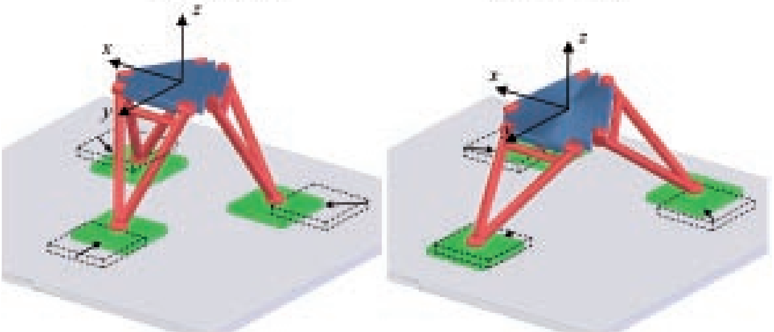

(c) z-translation (d) Rx-rotation

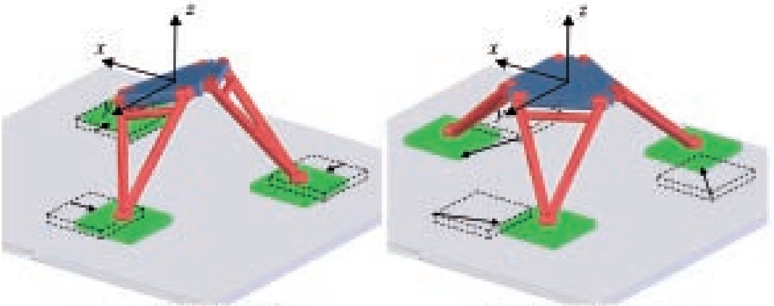

(e) Ry-rotation (f) Rz-rotation

Figure 3. Each of the independent six DoFs of the platform are created by combinations of planar *xy*-displacements of the three intermediate bodies.

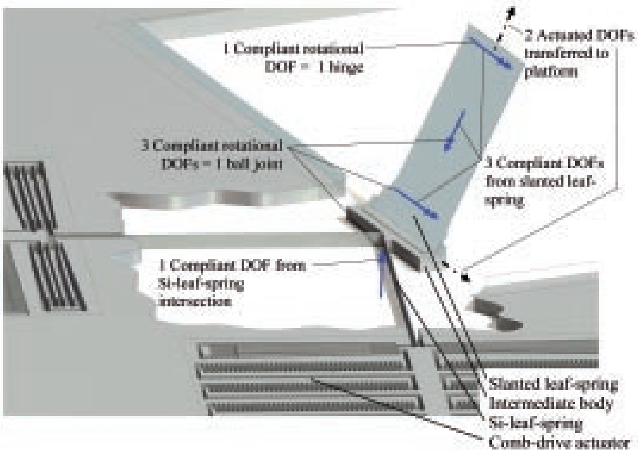

Figure 4. The six DoFs (two actuated and four compliant) of the platform defined by one leg. The slanted leaf-spring releases three DoFs. The intersection of the Si-leaf-springs releases one DoF. The three compliant DoFs near the intermediate body can be regarded as a ball joint, equivalent to the ball joint in Figure 2. The compliant DoF near the platform can be regarded as the hinge equivalent of Figure 2.

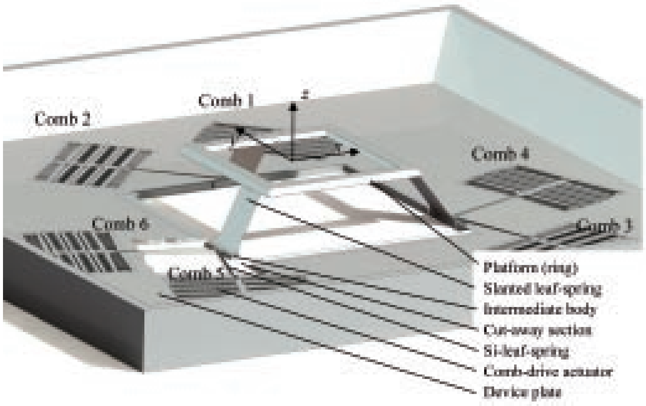

Figure 5. The MEMS-based 6-DoFs manipulator design. For viewing purposes a section has been cut away.

Fabrication process design

Five lithographic mask transfer steps are used in the total of 126 process steps. The concept is based on etching a 460 μm high pyramid in a 500 μm thick wafer, on which slanted leaf-springs of Silicon-rich-Nitride (SiRN) are deposited as shown in Figure 6. The pyramid is subsequently etched away leaving the slanted leaf-springs. A pyramid with flat sides can be etched by KOH using compensation structures [10]. KOH etches silicon along <111> crystal planes. The shape of the slanted leaf-springs is structured by evaporation of aluminum through a shadow mask and subsequently etching the leaf-springs. The comb-drives are etched by DRIE. The pyramid inside is etched by Reactive Ion Etching leaving the leaf-springs.

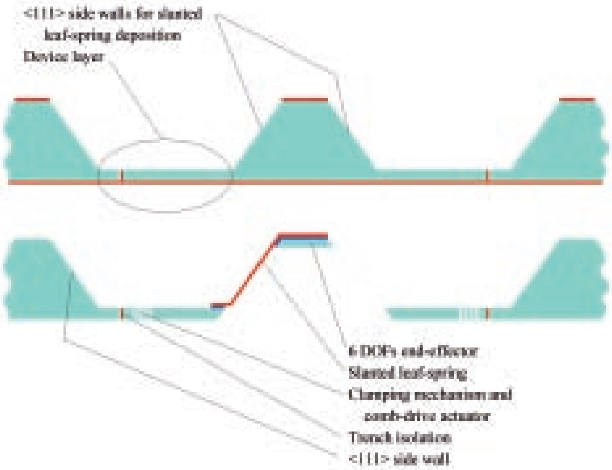

Figure 6. Brief overview of the fabrication of the 6-DoFs MEMS-based precision manipulator. Top figure shows a cross-section of the manipulator after KOH etching. Bottom figure shows the cross-section of the manipulator after the total processing.

Modeling the manipulator

Based on dimensions of the elastic elements, the folded flexures, the slanted leaf-springs and the Si-leaf-springs, the manipulator is modeled. An estimation of the actuation force and stroke can be made using a software package called SPACAR. SPACAR considers elastic elements as multi-body-like finite elements, which considerably reduces the number of elements, which makes the analysis fast and effective [11]. The typical relatively large deformations of elastic hinges in MEMS result in relatively large displacements and large rigid body rotations. Geometrically non-linear elasticity theory is a necessity for accurate analysis.

To reach the specified translations in all directions and small correctional rotations at the same time, the actuators need displacements of about 50 μm in two directions. This actuator stroke is rather large, which is due to the parallel kinematic manipulator set-up. The ‘individual platform displacements’ are about five times larger than the ‘combined platform displacements’, with the same actuator strokes.

Therefore, in a first fabrication design of the manipulator the displacements of the comb-drives are limited to reduce risk. At a stroke of 20 µm the most demanding actuator needs to deliver 275 µN. For MEMS this calculated force is rather large. In comparison to slanted and Si-leaf-springs, the folded flexures are relatively stiff in the actuation direction consuming 80 to 100% of the actuator force. This is partly a consequence of the necessity to have a high *z*-stiffness of the platform and the large force leverage by the Si-leaf-springs from the platform to the folded flexures. The lowest vibration mode frequencies and the accompanying vibration modes have been calculated. Figure 7 shows the first vibration mode with blocked actuators. The first three vibration mode frequencies with blocked actuators are calculated to be 3.8 to 4.4 kHz with accompanying motions of the platform mainly in the *z*-direction. The vibration modes are mainly caused by the out-of-plane of the wafer bending of the Si-leaf-springs. However, the fourth vibration mode, with a much higher frequency of 18.2 kHz, is not caused by out-of-plane bending of the Si-leaf-springs. Therefore, if the out-of-plane bending stiffness of the Si-leaf-springs could be increased, the first three vibration mode frequencies would be increased considerably. This is caused by the limited height (35 µm) to thickness (3 µm) ratio of the Si-leaf-springs due to DRIE fabrication. A compromise had to be made between the preferably compliant and thus low-frequency unblocked actuation modes and the preferably high-frequent blocked actuator modes. This is essentially a trade-off between the necessary actuator force for displacing the platform and the first vibration mode frequency.

The stiffness of leaf-springs changes when deflected. Therefore, the vibration mode frequencies of the platform are expected to change when the platform is deflected as well. The frequency change of the mode is largest for a displacement in the *z*-direction. However, the change is only 3% at a *z*-displacement of 20 µm and is therefore not significant.

The stress by internal forces due to deflection is low. In general, this is the case if relatively low force actuators (comb-drives) are used in a compliant mechanism. The buckling load is the lowest in the *x*-direction on the platform, i.e. 0.21 mN. Stress caused by internal or external causes is not the failure mechanism for the manipulator, buckling is. This is the consequence of the long slender leaf-springs necessary to make the mechanism compliant enough for the low-force actuators to result in the required strokes. To prevent stress concentrations due to notches, which are critical in single crystal material, all corners are rounded.

There are several sources causing thermal noise in the manipulator: the electron beam, sources attached to the TEM column, and thermo-mechanical noise. No significant heating is caused by the electrostatic comb-drive actuators. Due to the interaction of the electrons with the sample, electrons lose about 0.02% of their energy. The electron beam heats the sample with about 20 nW. In a steady state of heat flow the maximum temperature difference between the sample and the platform will be 2.5 mK. The largest position change of the manipulator of 0.66 pm arises due to a 0.42 mK temperature increase of the slanted leaf-springs. The largest time constant of 1.9 s is small, which results in a fast adjustment of the sample and manipulator temperature to the TEM column temperature.

Thermo-mechanical noise is caused by the jiggles and jitters of matter having a finite temperature. Therefore, temperature is principally causing motion. Although a system might be in thermal equilibrium, the velocities of the molecules assume a huge range of values, but are not arbitrarily distributed. This thermal agitation of particles causes white noise and is called thermo-mechanical noise. At the micron scale the stiffness of a system can become so small that the small force fluctuation causes significant movement of the system. In AFM microscopes and in MEMS-based accelerometers this noise can be significant. However, because the stiffness of the platform is relatively high, the thermo-mechanical noise has no significant influence on the positional stability of the platform.

Conclusion and results

A design has been presented for a 6-DoFs MEMS-based precision manipulator. The necessary combination of in-plane and out-of-plane motion of the wafer in MEMS is rather new. The specifications for a precision manipulator require high-frequency vibration modes combined with compliant actuation modes. The compliant actuation modes are necessary to generate sufficient displacement of +/- 10 µm by the low force MEMS actuators. Therefore, the design principles, especially exact kinematic constraint design, have been applied as much as possible. However, trade-offs had to be made between what is required from an exact kinematic constraint design point of view and what is feasible with the available fabrication processes. Although the design incorporates relatively long and slender leaf-springs, the first vibration mode frequency is 3.8 kHz (with blocked actuators). However, the cleanroom fabrication of the total manipulator required more time than available during the project. Therefore, only several fabrication steps of the manipulator design have been tested.

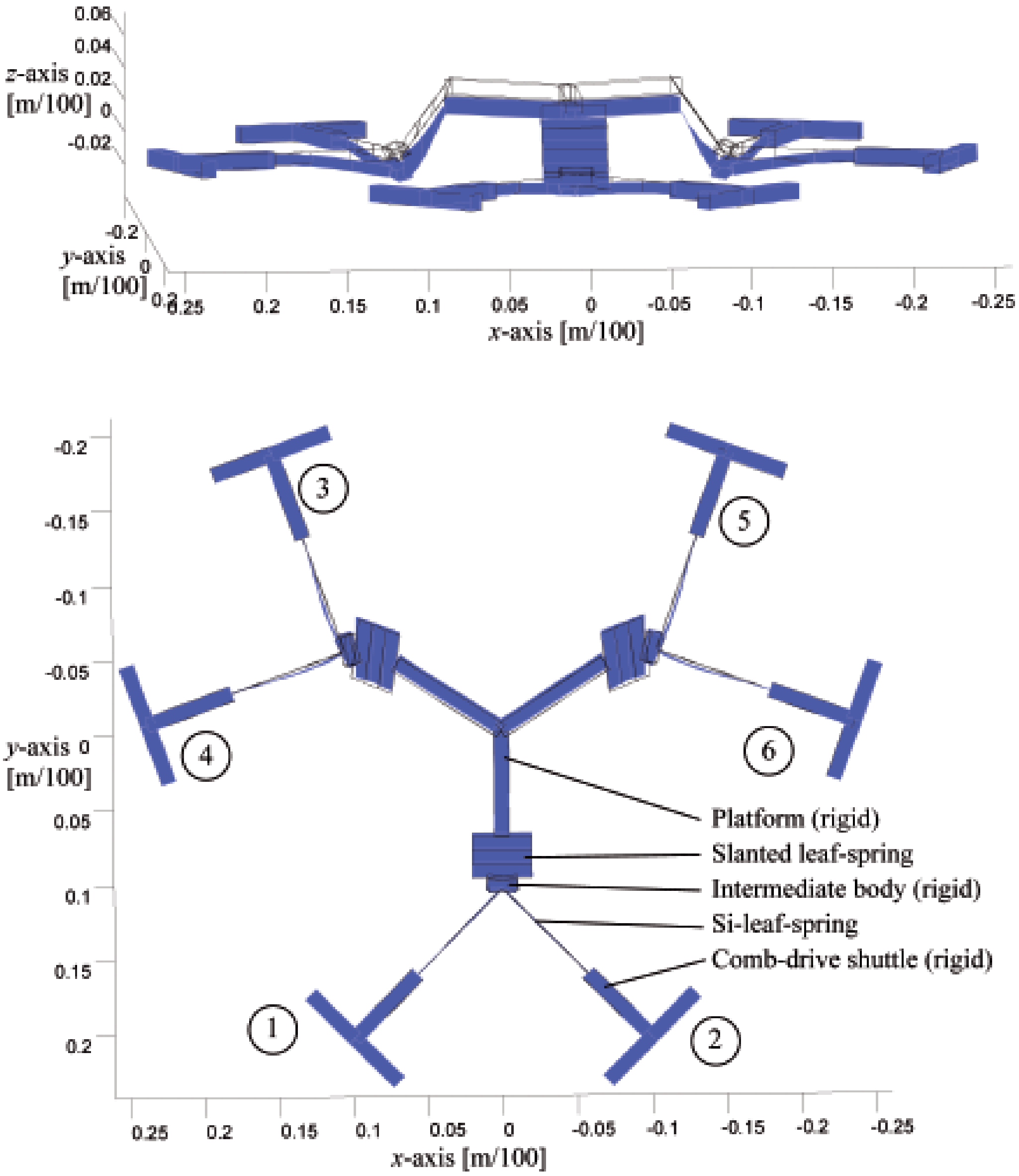

Figure 7. The first vibration mode with blocked actuators at 3.8 kHz. The platform mainly moves in the z-direction. The dimensions shown are used for viewing purposes only, they are not the real dimensions.

The overall conclusion on MEMS-based micro-mechatronic design is twofold:

- Precision design in MEMS is a synthesis of the fabrication process design and exact kinematic constraint design, requiring trade-offs.
- In MEMS-based precision design exact kinematic constraint design is a necessity to obtain both a high actuation compliance and high vibration mode frequencies of the suspension modes.

The research and manufacturing of a MEMS-based multi-DoFs precision manipulator with integrated feedback will be continued in a new Point-One project called CLEMPS (Closed-Loop Embedded MEMS-based Precision Stage), which is currently conducted by the University of Twente, DEMCON and FEI Company.

Acknowledgement

The research described in this article is part of the Multi Axes Micro Stage (MAMS) project and has been conducted in the chair of Mechanical Automation and Mechatronics of the department of Mechanical Engineering within the IMPACT research institute at the University of Twente, Enschede, the Netherlands. The research has been financially supported by the Innovation Oriented research Programme (IOP) Precision Technology from the Dutch Ministry of Economic Affairs.

Special acknowledgement should be given to J.B. Jonker, J. van Dijk and R.G.K.M. Aarts. They enabled the extensive calculations in Spacar. Thanks to the collaboration with the Transducer Science and Technology group of M.C. Elwenspoek, design and fabrication of MEMS devices was made possible. Therefore special thanks to B.R de Jong, G.J.M. Krijnen, and M.J. de Boer.

Author's note

Dannis Brouwer is assistant professor in the department of Mechanical Engineering at the University of Twente and project manager with DEMCON in Oldenzaal. Herman Soemers is professor of Mechatronic Design at the University of Twente and senior mechatronics system designer with Philips Applied Technologies in Eindhoven.

References

[1] D.L. Blanding, Exact Constraint: Machine design using kinematic principles, ISBN 0-7918-0085-7, 1999.
[2] L.C. Hale, Principles and Techniques for Designing Precision Machines, Ph.D thesis, Lawrence Livermore National Laboratory, Feb. 1999.
[3] R.V. Jones, Instruments and experiences, papers on measurement and instrument design, ISBN 0 471 91763 X, 1988
[4] M.P. Koster, Constructieprincipes voor het nauwkeurig bewegen en positioneren, Twente University Press, ISBN 903651455x.
[5] P. Schellekens, N. Rosielle, H. Vermeulen, M. Vermeulen, S. Wetzels, W. Pril, Design for precision: current status and trends, Cirp. annals, Vol. 47/2/1998, pp.557-586.
[6] A.H. Slocum, Precision Machine Design, Prentice Hall, Englewood Cliffs, New Jersey, 1992.
[7] S.T. Smith, D.G. Chetwynd, Foundations of Ultra-Precision Mechanism Design, Developments in Nanotechnology, Vol 2, ISBN 2-88449-001-9, 1992.
[8] M.J. Madou, Fundamentals of Microfabrication, ISBN 0-8493-9451-1, 1997.
[9] E. Sarajlic, M. J. De Boer, H. V. Jansen, N. Arnal, M. Puech, G. Krijnen, and M. Elwenspoek, Bulk micromachining technology for fabrication of two-level MEMS in standard silicon substrate, in Transducers'05, vol. 2, Seoul, Korea, pp. 1404–1405, 2005.
[10] M. Bao, C. Burrer, J. Esteve, J. Bausells, S. Marco, Etching front control of <110> strips for corner compensation, Sensors and Actuators A, 37-38, (1993), pp. 727-732.
[11] J.B. Jonker, J.van Dijk and R.G.K.M. Aarts, An extended input-output representation for control synthesis in multibody system representation for control synthesis in multibody system dynamics, Multibody Dynamics 2007, Eccomas Thematic Conference, Milano, Italy, 25-28 June 2007.

Information

www.impact.utwente.nl